

## Central European Journal of Chemistry

# The computational modelling of the kinetics of ascorbic acid palmitate hydrolysis by lipase considering diffusion

#### Research Article

Jurgita Dabulytė-Bagdonavičienė<sup>1,2\*</sup>, Feliksas Ivanauskas<sup>2</sup>, Valdemaras Razumas<sup>3</sup>

> <sup>1</sup>Department of Applied Mathematics, Kaunas University of Technology, LT-51368 Kaunas, Lithuania

> > <sup>2</sup>Department of Computer Science, Vilnius University, LT-03225 Vilnius, Lithuania

<sup>3</sup>Institute of Biochemistry, Vilnius University, LT-08662 Vilnius, Lithuania

#### Received 25 October 2010; Accepted 2 April 2011

Abstract: This paper presents mathematical and computational modelling of kinetics of a bioelectroanalytical system based on the interfacial action of hydrolytic enzyme. A system of non-linear differential equations with diffusion is used to describe the kinetics of *Termomyces lanuginosa* lipase (TLL) catalyzed hydrolysis of L-ascorbic acid palmitate (AAP). The system was solved numerically, and the kinetic prameters of AAP hydrolysis by the enzyme were determined. The experimental and modelling results show linear dependence of the rate of AAP hydrolysis on the TLL concentration. Complex dependence of the initial rate of bioelectrocatalytic current increase on the thickness of total diffusion layer (hydrodynamic diffusion layer plus thickness of dialysis membrane on the electrode surface) is also demonstrated and explained.

**Keywords:** Ascorbic acid • Lipase • Enzyme reaction • Mathematical model • Computational model © Versita Sp. z o.o.

## 1. Introduction

Oxidative stress, arising as a result of an imbalance between free radical production and antioxidant defence systems, is associated with diseases [1-3]. L-Ascorbic acid (AA) is the most abundant non-enzymatic antioxidant which efficiently scavenges reactive oxygen species [1]. However, since AA is water soluble, the body faces problems absorbing it. To overcome this problem, AA can be chemically modified by esterification of the hydroxyl group(s) by acid(s). For example, L-ascorbic acid palmitate (6-O-palmitoyl-L-ascorbic acid; AAP) is not water soluble, and, consequently, it can be stored in cell membranes until it is required [4]. This makes AAP a very attractive form of vitamin C supplementation, e.g. as food preservative E304, and in the formulations of cosmetic and related products. However, so far, quite a few methods, either chromatographic or electrophoretic, for the analytical determination of AAP have been suggested [5,6]. This prompted some of us to develop

a novel electrochemical AAP assay system based on the amperometric detection of the enzymatic hydrolysis product [7].

The principle of the assay is as follows. AAP that contains both the ester and the electroactive AA-based groups is used as a Thermomyces lanuginosus lipase (TLL) substrate (see Scheme 1). It is also expected that the direct substrate oxidation will be significantly suppressed because the AAP molecules are solubilized in the Triton X-100 micelles, while the product of enzymatic hydrolysis, AA, could be readily oxidized to dehydroascorbic acid (DAA) on the electrode (Scheme 1). Additionally, to avoid direct oxidation of AAP on the electrode, and to reduce possible contamination of the electrode by the surfaceactive components of the solution, the electrode surface was covered by the dialysis membrane. The generated AA is oxidized on the surface of a gold electrode modified by a redox-active self-assembled monolayer (SAM). It has been shown that 9-mercaptononyl-5'ferrocenylpentanoate (FcC,H,COOC,H,SH) exhibits excellent electron mediator properties in the process of

the electrochemical oxidation of AA [8-10], which can potentially be utilized for the quantitative determination of AA. The catalytic current of AA oxidation serves as an indicator of the process intensity, which is proportional to both substrate concentration (in the present case, AAP) and enzyme activity. Thus, in conjunction with AAP, this electroanalytical system might be used for the determination of TLL activity. This is also important since lipases, triacylglycerol hydrolases (EC 3.1.1.3) that cleave triacylglycerols at the oil/water interface, have extensive applications in the food, paper, pharmaceutical, cosmetic, detergent, leather, and textile industries [11]. We note that a number of amperometric systems for the determination of TLL activity have been recently developed and modelled by some of us [12-14].

However, this study addresses mathematical and computational modelling of above- indicated bioanalytical systems. For this purpose, as in the case of our earlier study [14], the universally accepted model of enzyme kinetics in heterogeneous systems by Verger et al. [15] was applied. The model is described in detail in the experimental section of this study. Here, it should be pointed out that, in order to simplify the kinetic treatment of the model, two assumptions were made in [15]. First, it is assumed that the volume occupied by the substrate molecules which constitute the interface is negligible as compared to the total volume of the system. Second, it is inferred that the area occupied by the enzyme at the substrate interface is negligible by comparison with the total interfacial area. Clearly, for the micelle-based systems, the first assumption might be invalid at high micelle concentrations.

# 2. Experimental Procedure

#### 2.1. Physical model of the system

In this study, the rate of bioelectrocatalytic oxidation of AAP in terms of the catalytic current increase rate  $(dl_{ca}/dt)$  was examined vs. the concentration of TLL in

the bulk solution. Here, it is important to realize that, in the case of our system where the substrate forms micelles, the substrate surface concentration ( $[S]_0$ ) is a constant (the same is valid, for instance, in the case of emulsions). Therefore, a classical Michaelis-Menten relation between the rate of enzyme reaction and substrate concentration (in our case, between  $dI_{cal}/dt$  and  $[S]_0$ ) cannot be examined properly using experimental and theoretical methods. For a given substrate, its surface concentration depends only on the physical parameters of the solution (e.g. pH, ionic strength, and/or temperature). Another alternative is the measurements of enzymatic velocity as a function of micelle concentration. Unfortunately, we do not have such experimental results at our disposal.

The details pertaining to the electrochemical measurements are presented in [7]. Here, we provide only the most important aspects and parameters of experiments. Electrochemical measurements were performed at 40°C using a VersaStat (EG&G) computerized potentiostat system (Princeton Applied Research, Princeton, USA) with a rotating disk electrode (BAS RDE-2, USA) in a three electrode cell where the working electrode was gold (electrochemically active surface area of ca. 0.08 cm<sup>2</sup>, BAS, USA), the auxiliary electrode - Pt wire, and the reference saturated by sodium chloride Ag/AgCl electrode. Prior to experiments, the working electrode was modified by FcC,H,COOC,H,SH-based SAM (FcC,H,COOC,H,SH - synthesized at the Institute of Biochemistry). For this purpose, the gold electrode surface was polished on 0.05 µm alumina slurry (Struers, Denmark), sonicated for 5-10 min in a 1:1 mixture of water and ethanol, etched in aqua regia for 2 min, sonicated in water and potentiostatically scanned (100 mV s-1) in 1 M H<sub>2</sub>SO<sub>4</sub> solution in the potential (E) range between 0.0 and 1.5 V. After rinsing with water and ethanol, the electrode was transferred into the 0.1 mM solution of FcC<sub>4</sub>H<sub>8</sub>COOC<sub>9</sub>H<sub>18</sub>SH in ethanol and incubated for 12-15 h (for more details, see [8-10]). Following the chemical modification of the electrode surface, it was

**Scheme 1.** Enzymatic and electrochemical processes for the electrochemical determination of ascorbic acid palmitate and Termomyces lanuginosus lipase activity.

covered by the dialysis membrane of ca. 3×10-2-cm thickness. During measurements, the working electrode E = 0.4 V (vs. Ag/AgCl reference electrode), electrode rotation speed - 10.5 s<sup>-1</sup>.

Solutions were prepared in 0.01M sodium phosphate buffer (pH = 7.0, 40°C), containing 0.1 M NaCl, 5 mM NaClO, and 0.25% Triton X-100. The Triton (from Ferak, Germany) concentration of ca. 4 mM (= 0.25%) is much higher than the critical micelle concentration (CMC) of 0.08 mM [7]. Under these experimental conditions, the radius of micelle is equal to ca. 5.4 nm, whereas the aggregation number is close to 150 [16]. AAP was from Fluka (CMC = 0.1 mM [7]). In brief, determination of CMC of Triton X-100 and AAP were done using a UV-VIS spectrophotometer (PerkinElmer, Model Spectrum GX). The method was proposed by P. Becher [17]. Thus, the dye benzopurpurin 4B was dissolved (0.005%) in 0.01 M phophate buffer, containing 0.1 M NaCl (pH = 7.0). The Triton X-100 concentration was varied between 0.004 to 1.6 mM. From the differential absorbance at 500 nm as a function of the concentration logarithm, the CMC of Triton X-100 was determined at 40°C. The CMC value of AAP was determined in an analogous manner and was found to be 0.105(±0.006) mM at 40°C (in the experiments, the AAP concentration was varied between 0.004 to 1.4 mM).

TLL was from Sigma (concentration range used in the experiments - from 14 to 59 µM). The activity of lipase was 0.18(±0.04) U per mg of enzyme preparation as determined spectrophotometrically with respect to the hydrolysis of 4-nitrophenylpalmitate. For the measurements, the initial concentrated solution of TLL was used (70 mg mL-1 as deduced from the UV absorption at 260 and 280 nm, molecular weight 29 kDa).

Scheme 2 presents a model for the kinetic description of lipase action at the interface, proposed by Verger et al. [15]. This model consists basically of three successive stages. The first step describes the reversible penetration of a water-soluble enzyme into an interface region. To be consistent with the fact that the enzyme reaction occurs at the interface, the concentration of penetrated enzyme must be expressed in a two-dimensional way. that is to say, in moles (or molecules) per unit surface area. After this step of penetration, which leads to the penetrated enzyme  $E^*$ , follows a second equilibrium, giving a kind of "interfacial Michaelis-Menten complex" [15,18,19]. This complex, denoted by  $E^*S$ , is formed by the combination of a single substrate molecule with the penetrated enzyme. This is the equivalent in two dimensions of the classical Michaelis-Menten equilibrium. Once the complex  $E^*S$  is formed, the catalytic step takes place regenerating enzyme in the form  $E^*$  along with the formation of the products – AA and palmitic acid. In this paper, we consider only the situation when the whole of the redox-active reaction product (AA) dissolves in the water phase, and, because of the rotating disc electrode action, diffuses rapidly away from the micelle interface.

#### 2.2. Mathematical model

Mathematically, the kinetics of the above-mentioned model (Scheme 2) is defined by the system of equations

$$[E]_0 = [E] + [E^*] \cdot \frac{I}{V} + [E^*S] \cdot \frac{I}{V}, \tag{1}$$

$$\frac{d[E^*S]}{dt} = k_1[E^*][S] - (k_2 + k_{-1})[E^*S], \qquad (2)$$

$$\frac{d[E^*]}{dt} = k_p[E] + (k_2 + k_{-1})[E^*S] - (k_d + k_1[S])[E^*], \qquad (3)$$

$$\frac{d[E^*]}{dt} = k_p[E] + (k_2 + k_{-1})[E^*S] - (k_d + k_1[S])[E^*], \quad (3)$$

$$\frac{\partial [P]}{\partial t} = D \cdot \frac{\partial^2 [P]}{\partial x^2} + k_2 [E^* S] \cdot \frac{I}{V}, (x, t) \in \Omega, \tag{4}$$

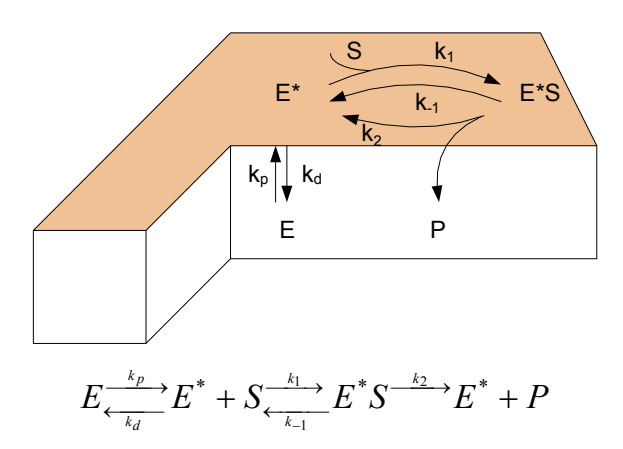
where [E] (mol cm<sup>-3</sup>),  $[E^*]$  $[E^*S]$  (mol cm<sup>-2</sup>), [S] (mol cm<sup>-2</sup>), [P] (mol cm<sup>-3</sup>) represent the concentrations of the substances indicated,  $[E]_{b-1}$ the total enzyme concentration (mol cm $^{-3}$ ), I – the total interfacial area of micelles (cm2), V - the total volume of solution in the electrochemical cell (cm $^3$ ), D - the diffusion coefficient of P (cm<sup>2</sup> s<sup>-1</sup>), t – the time (s), x- the space coordinate (cm), and for  $\Omega = \Omega_1 \cup \Omega_2 \cup \Omega_3$  see Scheme 3 below.

In the one-dimensional model (Scheme 3), the working space of the system described by Eqs. 1-4 could be presented as a wide area of a diffusion layer r, where the diffusion of hydrolysis product occurs.

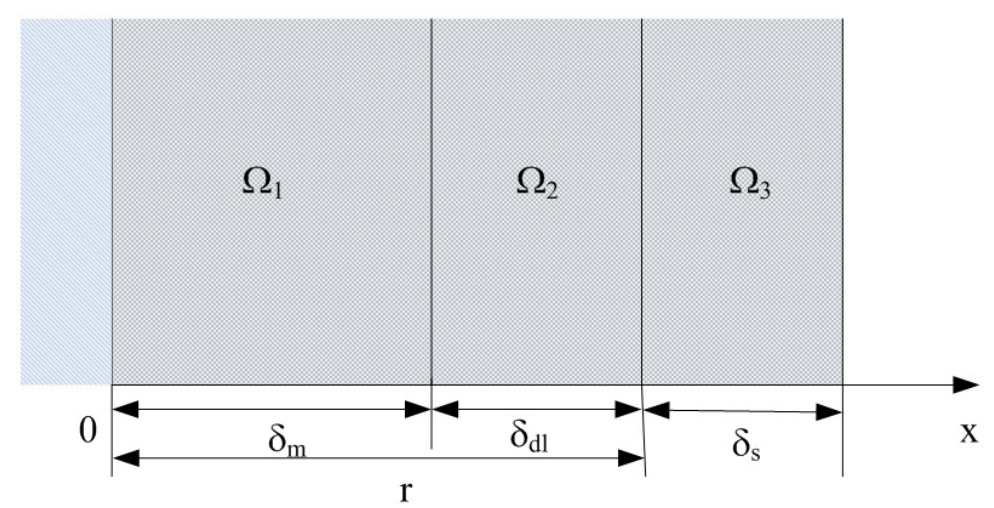
According to Eqs. 1-4, only the diffusion of Ptakes place in area  $\Omega_1 \cup \Omega_2$ , generating amperometric response of the system. In areas  $\Omega_1$ ,  $\Omega_2$ , and  $\Omega_3$ , Eq. 4 should be rewritten as

$$\frac{\partial[P]}{\partial t} = \begin{cases}
D_m \cdot \frac{\partial^2[P]}{\partial x^2} + k_2[E^*S] \cdot \frac{I}{V}, & x \in \Omega_1, \\
D_{dt} \cdot \frac{\partial^2[P]}{\partial x^2} + k_2[E^*S] \cdot \frac{I}{V}, & x \in \Omega_2, \\
k_2[E^*S] \cdot \frac{I}{V}, & x \in \Omega_3,
\end{cases} \tag{5}$$

where  $D_m$  - the diffusion coefficient of P in the dialysis membrane,  $D_{dl}$  - the diffusion coefficient of P in the hydrodynamic diffusion layer. Since diffusion does not occur in area  $\Omega_3$ , and, therefore, the concentrations are the same in the whole area, it is enough to set a suitable boundary condition for x = r, not analysing  $\Omega_3$ . The electrical signal is proportional to the derivative of reaction product concentration  $\frac{\hat{o}[P]}{\hat{o}x}\Big|_{z=0}$ . Namely, the change of this parameter with time is one of the objects of our computational study.



Scheme 2. The model of interfacial enzyme reaction catalyzed by TLL (adapted from [15]), where *E* – the free enzyme in solution, *E*\* – the penetrated enzyme at the surface of micelle, *E*\*S – the penetrated enzyme-substrate complex, *S* – the substrate (AAP) entrapped in Triton X-100 micelles, *P* – the redox-active reaction product (AA), *k*<sub>ρ</sub> – the penetration rate constant, *k*<sub>1</sub> – the rate constant of *E*\*S complex formation, *k*<sub>.1</sub> – the rate constant of *E*\*S complex decomposition, *k*<sub>2</sub> – the catalytic rate constant.



**Scheme 3.** The schematic view of the model used in the present study:  $\Omega_1 \cup \Omega_2$  - area, where diffusion of reaction product (AA) occurs,  $\Omega_3$  - the area of solution, x=0 - the electrode surface,  $\delta_m$  - the thickness of dialysis membrane,  $\delta_{dl}$  - the thickness of the hydrodynamic diffusion layer,  $\delta_s$  - the thickness of solution.

The investigation of the system of Eqs. 1-3, and 5 can be divided into two steps. The system of non-linear Eqs. 1-3 can be solved first, and later, partial differential Eq. 5 can be solved using the  $E^*S$  concentration as the solution of the above—mentioned system.

The following initial conditions (t = 0) are applied:

$$[E]_{0}(0) = [E]_{0}, \quad [E]_{0}(0) = 0,$$
  
 $[E^{*}]_{0}(0) = 0, \quad [E^{*}S]_{0}(0) = 0,$  (6)  
 $[S]_{0}(0) = [S]_{0}$ .

The initial condition for the second part of calculations is

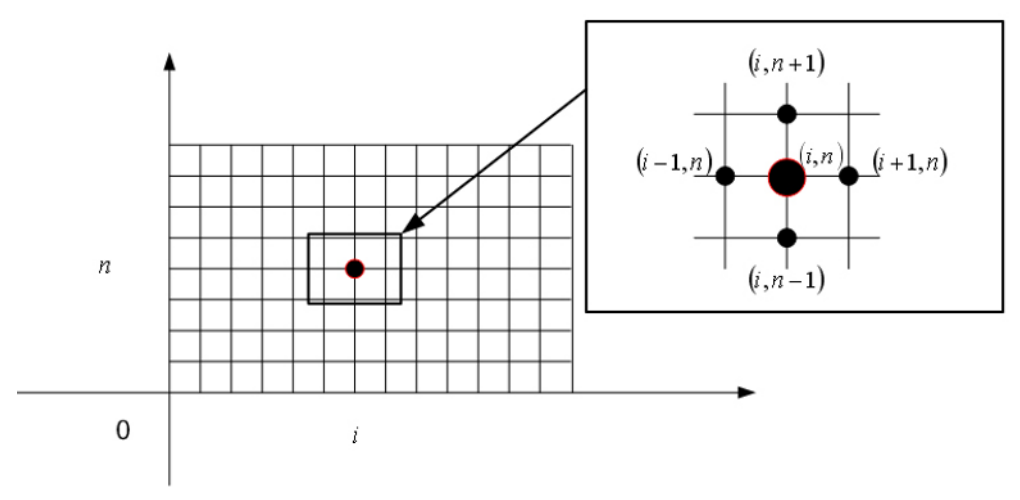
$$[P](x,0)=0, \quad x \in [0,r]$$
 (7)

whereas the boundary conditions are:

$$\begin{split} & [P](0,t) = 0, \qquad t > 0, \\ & D_m \cdot \frac{\partial [P](x,t)}{\partial x} \bigg|_{x = \delta_m} = D_{dl} \cdot \frac{\partial [P](x,t)}{\partial x} \bigg|_{x = \delta_m}, \qquad t > 0, \quad (8) \\ & \frac{\partial [P](x,t)}{\partial x} \bigg|_{x = r} = k_2 [E^*S] \cdot \frac{I}{V}, \quad t > 0. \end{split}$$

The initial rate of AAP bioelectrocatalytical current increase can be found using an expression for the steady-state current of membrane-covered rotating disc electrode from [20] and multiplying it by  $\frac{\partial [P]}{\partial t}$ :

(7) 
$$\frac{dI_{cat}}{dt} = 0.62 n_e FAD_{dl}^{2/3} \omega^{1/2} v^{-1/6} \cdot \frac{1}{1 + \frac{P_t}{P_m}} \cdot \frac{\partial [P]}{\partial t}, \qquad (9)$$



Scheme 4. The schematic view of discrete mesh.

where  $n_e$  – the number of electrons, F – the Faraday constant, A – the surface area of electrode,  $\omega$  – angular rotation speed of electrode,  $\nu$  – the kinematic viscosity of solution,  $P_t = D_{dl}/\delta_{dl}$  – permeability of the solution,  $P_m = \alpha D_m/\delta_m$  – permeability of the membrane,  $\alpha$  - the ratio of ascorbic acid concentrations in the membrane and solution,  $\partial [P]/\partial t$  – the rate of AAP hydrolysis by TLL,  $I_{cat}$  – the catalytic current.

At this juncture, it should be pointed out that most scientific and engineering problems are comprised of complex geometries and loading configurations, *i.e.*, complicated mathematical models, making an analytical solution impossible. In order to achieve a solution, a numerical solution technique must be employed. Therefore, our mathematical model is solved numerically [21]. The finite—difference technique and its implicit scheme is used for the discretization of the present model. In literature, a similar approach to mathematical and computational modelling using analogous schemes is under active consideration [22-25].

Let us denote the scope  $\Omega$ :

$$\Omega = \{ (x,t) : 0 < x < r, 0 < t \le T \}.$$

The discrete mesh is described in the area  $\,\Omega\,.$  Discretization of the spatial coordinate gives:

$$W_h = \{x_i = h, i = 1, 2, ..., N-1, h = r/N\},\$$

$$\overline{w}_h = w_h \cup \{x_0, x_N\}$$

and discretization of the time coordinate yields:

$$w_{\tau} = \{ t^{n} = n\tau, n = 1, 2, ..., K, t^{K} = T \}$$

$$\overline{w}_{\tau} = w_{\tau} \cup \{ t^{0} \},$$

where h is the step in space and  $\tau$  is the time step. The discrete mesh is the set of  $w_{h\tau} = w_h \times w_\tau$ . All points of this set are divided into subsets  $\overline{w}_{h\tau} = w_{h\tau} \times \gamma_{h\tau}$ . The points of set  $w_{h\tau} = w_h \times w_\tau$  are called the inner points of the discrete mesh and the

points of the set  $\gamma_{h\tau} = (\{0, r\} \times w_{\tau}) \cup (w_h \times \{t^0 = 0\})$  are called the boundary points of the discrete mesh.

The j<sup>th</sup> layer of the discrete mesh is composed of all the points with the same time coordinate  $w(t^j) = \{x_i, t^j\} i = 0, 1, 2, ..., N \}$  (Scheme 4).

Let us denote the functions and derivatives (by using forward difference approximation of first derivative and second partial derivative approximation) defined in the points of discrete mesh  $\overline{w}_{h\tau}$ :

$$\begin{split} & [E]_0(t) = [E]_0(t^n) = [E]_0 \ ^n, & [E]_t(t) = [E]_t(t^n) = [E] \ ^n, \\ & [E^*]_t(t) = [E^*]_t(t^n) = [E^*] \ ^n, & [E^*S]_t(t) = [E^*S]_t(t^n) = [E^*S] \ ^n, \\ & [S]_t(t) = [S]_t(t^n) = [S] \ ^n, & [P]_t(x,t) = [P]_t(x_t,t^n) = [P]_t \ ^n, \\ & [E^{\hat{+}}S] = [E^*S]_t^{n+1}, & [\hat{E}^*] = [E^*]_t^{n+1}, & [\hat{E}] = [E]_t^{n+1}, & [\hat{P}]_t = [P]_t^{n+1}, \\ & \frac{d[E^*S]}{dt} \cong \frac{[E^{\hat{+}}S] - [E^*S]}{\tau}, & \frac{d[E^*]}{dt} \cong \frac{[\hat{E}^*] - [E^*]}{\tau}, & \frac{\partial [P]}{\partial t} \cong \frac{[\hat{P}]_t - [P]_t}{\tau}, \\ & \frac{\partial^2 [P]}{\partial x^2} \cong \frac{[P]_{t+1} - 2[P]_t + [P]_{t-1}}{h^2}. \end{split}$$

In the inner point of the discrete mesh, the system of differential Eqs. 1-3 is approximated by the system of finite difference equations:

$$[E]_{0} = [\hat{E}] + [\hat{E}^{*}] \frac{I}{V} + [\hat{E}^{*}S] \frac{I}{V}, \qquad (10)$$

$$\frac{\left[\underline{E^*S}\right] - \left[E^*S\right]}{\tau} = k_1 \cdot \left[\hat{E}^*\right] \left[\hat{S}\right] - \left(k_2 + k_{-1}\right) \left[E^*S\right], \tag{11}$$

$$\underbrace{\left[\stackrel{\wedge}{E^*}\right] - \left[E^*\right]}_{\tau} = k_p \cdot \left[\stackrel{\wedge}{E}\right] + \left(k_2 + k_{-1}\right) \left[E^*S\right] - \left(k_d + k_1 \left[\stackrel{\wedge}{S}\right]\right) \left[\stackrel{\wedge}{E^*}\right]. (12)$$

The concentrations of the elements taking part in the process in every time layer fulfill the following system of equations:

$$[\hat{E}] + [\hat{E}^*] \frac{I}{V} + [\hat{E}^*S] \frac{I}{V} = [E]_0,$$
 (13)

$$-\tau \cdot k_{1} \cdot [\hat{E}^{*}] [\hat{S}] + (1 + \tau (k_{2} + k_{-1})) [\hat{E}^{*}S] = [E^{*}S], \tag{14}$$

$$-\tau \cdot k_p \cdot \left[\hat{E}\right] + \left(1 + \tau \cdot \left(k_d + k_1 \left[\hat{S}\right]\right)\right) \left[\hat{E}^*\right] - \tau \cdot \left(k_2 + k_{-1}\right) \left[\hat{E}^*S\right] = \left[E^*\right]. \tag{15}$$

The initial conditions for obtaining the solution are:

$$[E]_0^0 = [E]_0, [E]_0^0 = 0, [E^*]_0^0 = 0, [E^*S]_0^0 = 0, [S]_0^0 = [S]_0.$$
 (16)

Let us assume that the total enzyme concentration and substrate concentration do not vary with time, *i.e.*, [E], "=[E], [S] "=[S],  $n \in [0,T]$  In the case of S, this statement means that, over the time window of our experiment, TLL converts only insignificant portion of the micelle-immobilized AAP.

The solution of this system is used in the second part of our study: the calculations of [P]. Eq. 4 turns into the following numerical expression:

$$\frac{\left[\hat{P}\right]_{i} - \left[P\right]_{i}}{\tau} = D \cdot \frac{\left[\hat{P}\right]_{i+1} - 2\left[\hat{P}\right]_{i} + \left[\hat{P}\right]_{i-1}}{h^{2}} + k_{2} \cdot \left[\hat{E}^{*}S\right] \frac{I}{V}, \quad (17)$$

taking into account that D can be equal to  $D_m$  or  $D_{dl}$  depending on x ( $x \in \overline{0, \delta_m}$  or  $x \in \overline{\delta_m, r}$ ).

As can be seen from the ordered equation

$$-\frac{\tau \cdot D}{h^{2}} \cdot \left[\hat{P}\right]_{i+1} + \left(\frac{2\tau \cdot D}{h^{2}} + 1\right) \left[\hat{P}\right]_{i} - \frac{\tau \cdot D}{h^{2}} \cdot \left[\hat{P}\right]_{i-1} =$$

$$= \tau \cdot k_{2} \cdot \left[\hat{E}^{*}S\right] \frac{I}{L} + \left[P\right]_{i}, \tag{18}$$

the product concentration is analyzed in three mesh points, that is why the implicit difference scheme is used for obtaining AA concentration in all the points of the investigated area.

The initial product concentration is:

$$[P]_{i}^{0} = 0, \ i = \overline{0, N}.$$
 (19)  
And the boundary conditions are:

$$[P]_0^n = 0, \quad n > 0,$$

$$D_{m} \cdot \frac{[P]_{i}^{n} - [P]_{i-1}^{n}}{h} \bigg|_{i=\delta_{m}/N} = D_{dl} \cdot \frac{[P]_{i+1}^{n} - [P]_{i}^{n}}{h} \bigg|_{i=\delta_{m}/N}, \quad n > 0, \quad (20)$$

$$\frac{[P]_{N}^{n} - [P]_{N-1}^{n}}{h} = k_{2} [E^{*}S]^{n} \cdot \frac{I}{I}, \quad n > 0.$$

Corresponding to this scheme, the product concentration is obtained using the iterations method.

## 3. Results and Discussion

The simulation experiments were designed according to the model system comprised of Eqs. 1-3, and Eq. 5. As mentioned earlier, the calculations were divided into two steps: in the first step, the calculations were done according to Eqs. 1-3, and, in second step, the diffusion of the product was calculated. Computer simulation of the system under consideration was carried out with the following values of parameters:  $[E]_0 = 5.9 \times 10^{-8}$  mol cm<sup>-3</sup>,  $[S]_0 = 1.7 \times 10^{-11}$  mol cm<sup>-2</sup>,  $I = 4.7 \times 10^5$  cm<sup>2</sup> (calculated knowing the concentration and dimensions of micelles), V = 8.2 cm<sup>3</sup> (solution volume in the electrochemical cell),  $D_{cll} = 6.5 \times 10^{-6}$  cm<sup>2</sup> s<sup>-1</sup> [26],  $D_m = 6.5 \times 10^{-7}$  cm<sup>2</sup> s<sup>-1</sup>

(it is assumed that *D* in the membrane decreases tenfold),  $\delta_{dl} = 4.3 \times 10^{-3}$  cm (at  $\omega = 10.5$  s<sup>-1</sup> [27]),  $\delta_{m} = 3 \times 10^{-2}$  cm. In this study, we also assume that the parameter  $\alpha$  in Eq. 9 is equal to 1.

Unfortunately, because of the complexity of interfacial lipase action (see Scheme 2), all individual kinetic constants for these enzymes are generally not reported in the literature. In fact, individual rate constants of TLL action for a system similar to the one discussed in the present work were only reported previously in [14], where they were numerically determined. Therefore, those constants reported were the starting point in the current calculations. The final values of rate constants for the system analyzed in this study are:  $k_0 = 0.025 \text{ cm s}^{-1}, k_d = 100 \text{ s}^{-1}, k_1 = 2 \times 10^9 \text{ cm}^2 \text{ mol}^{-1} \text{ s}^{-1},$  $k_{-1}$  = 10 s<sup>-1</sup>,  $k_2$  = 84 s<sup>-1</sup>. The final values were found by solving the reverse problem: by knowing experimental results, the values for the rate constants of interest were optimized to give good correlation between the experimental and modelled results.

The system of differential equations was discretized using an implicit finite difference scheme and the system of non-linear equations, corresponding to this scheme, was solved using an iterative method. Integration steps in space and time were as follows:  $h_x = 0.00015$  cm, t = 0.01 s. The results of the computational experiment are presented in Fig. 1. The curves of product concentration vs. time are different only in the space interval  $x \in [0, r/4]$ .

The series of computational experiments were performed to investigate the effect of TLL concentration on the initial rate of AAP hydrolysis. For the membrane-coated rotating disc Au electrode, the initial rate of AAP bioelectrocatalytic oxidation current increase is calculated by Eq. 9 using the following additional parameters:  $n_e = 2$ ,  $F = 9.65 \times 10^4$  C mol<sup>-1</sup>,  $v=0.01 \,\mathrm{cm^2 s^{-1}}$  [27],  $A=0.08 \,\mathrm{cm^2}$ . Different initial rate values of current increase were obtained for the different values of total enzyme concentration at the same time (100 s), and Fig. 2 shows linear dependence as expected for the classical Michaelis-Menten reaction, and as demonstrated in [7]. Moreover, good correlation between the experimental and computational results is observed in Fig. 2.

In addition to the above results, Fig. 3 shows a nonlinear decrease of  $\frac{dI_{cat}}{dt}$  with increasing the thickness of the AA diffusion layer  $\delta_{dl}$ . The current is calculated near the electrode surface. These results clearly indicate that, over the  $\delta_{dl}$  interval analyzed in Fig. 3, the bioanalytical system operates under the mixed membrane and solution transport control. In the limiting case of solution transport control ( $\frac{P_{u}}{P_{m}} << 1$  in Eq. 9), the dependence of Fig. 3 should be linear, since  $\delta_{dl} = 1.6 D^{1/3} \nu^{1/6} \omega^{-1/2}$  [27].

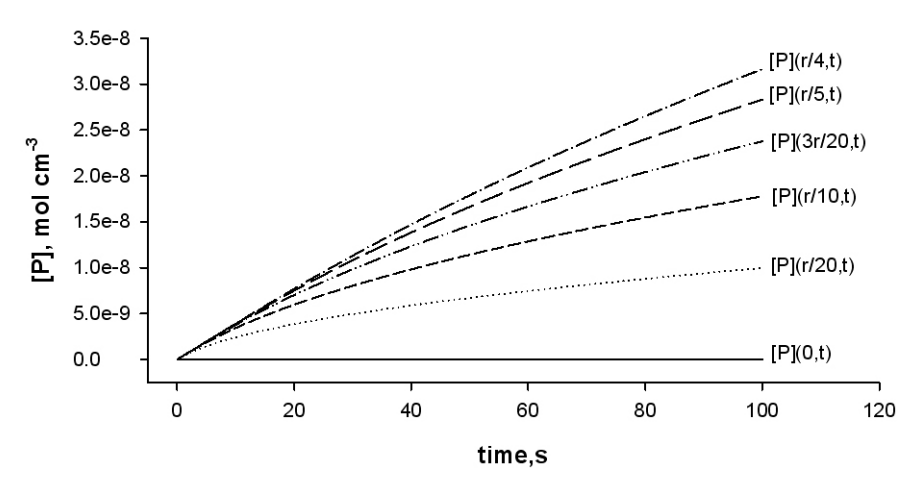


Figure 1. Product concentration increase with time at different space points. Starting from the point x = r/4 the obtained product concentration (data not shown) is the same as in the case of [P](r/4,t).

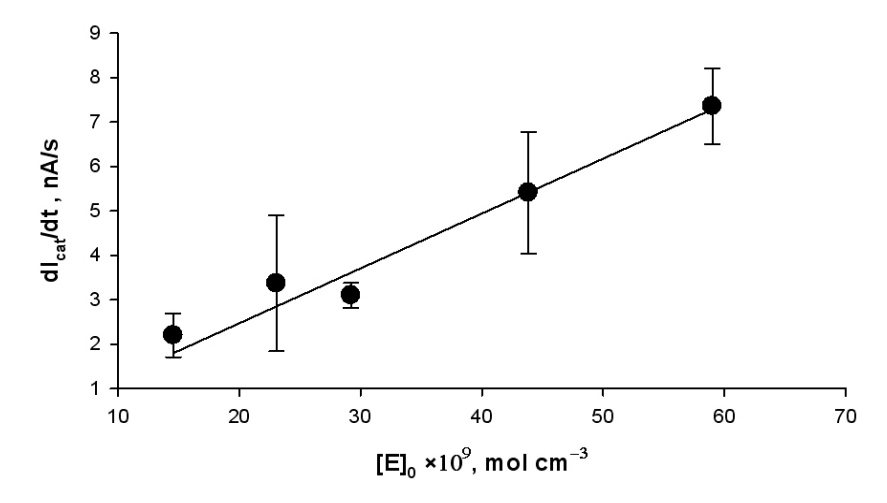
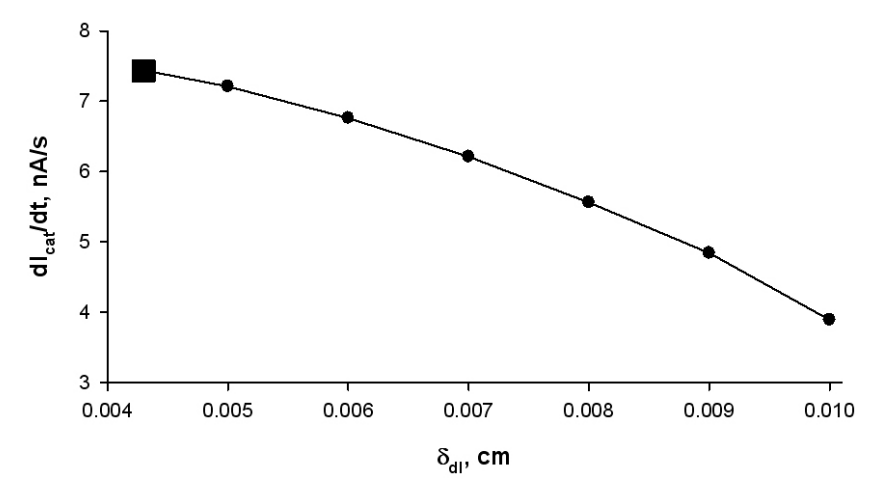


Figure 2. Dependence of the initial rate of AAP hydrolysis on the total TLL concentration. The solid line describes computed results, the filled circles with error bars – experimental data from [7]. For the experimental conditions, see Section 2 of this study. In both cases, [S]<sub>0</sub>=1.7×10<sup>-11</sup> mol cm<sup>-2</sup>



On the other hand, when  $\frac{P_t}{P_n} >> 1$ , the system operates under the membrane transport control, and the current should be independent of the value of  $\delta_{dl}$  [20].

## 4. Conclusions

In brief, we can summarize the results of our study by drawing the following conclusions:

1. Assuming a model consisting of a single diffusion layer at the membrane-coated electrode surface, we were able to compute the performance of the bioelectroanalytical system for the amperometric determination of ascorbic acid palmitate and *Thermomyces lanuginosus* lipase activity using the kinetic model of enzyme reaction developed by Verger et al. [16].

#### References

- [1] S.R. Pinnell, H. Yang, M. Omar, N.M. Riviere, H.V. DeBuys, L.C. Walker, Y. Wang, M. Levine, Dermatol. Surg. 27, 137 (2001)
- [2] Z. Tao, Y. Ren, W. Tong, D. Wei, Pharm. Rep. 57, 77 (2005)
- [3] D.L. Nelson, M.M. Cox, Leninger Principles of Biochemistry (Freeman, New York 2005)
- [4] M. Pokorski, M. Marczak, A. Dymecka, P. Suchocki, J. Biomed. Sci. 10, 193 (2003)
- [5] E. Sottofattori, M. Anazaldi, A. Balbi, G. Tonelio, J. Pharm. Biomed. Anal. 18, 213 (1998)
- [6] C.C. Wang, A.M. Wu, Anal. Chim. Acta, 576, 124 (2006)
- [7] B. Kazakevičienė, PhD thesis, Institute of Biochemistry (Publishing House of Vilnius University, Vilnius, 2006) (in Lithuanian)
- [8] B. Kazakevičienė, G. Valinčius, G. Niaura, Z. Talaikytė, M. Kažemėkaitė, V. Razumas, J. Phys. Chem. B 107, 6661 (2003)
- [9] G. Valinčius, G. Niaura, B. Kazakevičienė, Z. Talaikytė, M. Kažemėkaitė, E. Butkus, V. Razumas, Langmuir 20, 6631 (2004)
- [10] B. Kazakevičienė, G. Valinčius, G. Niaura, Z. Talaikytė, M. Kažemėkaitė, V. Razumas, D. Plaušinaitis, A. Teišerskienė, V. Lisauskas, Langmuir 23, 4965 (2007)
- [11] A. Houde, A. Kademi, D. Leblanc, Appl. Biochem. Biotech. 118, 155 (2004)
- [12] G. Valinčius, I. Ignatjev, G. Niaura, M. Kažemėkaitė, Z. Talaikytė, V. Razumas, A. Svendsen, Anal. Chem. 77, 2632 (2005)
- [13] I. Ignatjev, G. Valinčius, I. Švedaitė, E. Gaidamauskas. M. Kažemėkaitė, V. Razumas,

- 2. Good correlation between the linear experimental and computational results for the dependence of the rate of ascorbic acid palmitate hydrolysis on the enzyme concentration has been demonstrated.
- 3. The results of our study also indicate that, over the interval of hydrodynamic layer thickness analyzed, *i.e.*, from 0.0043 to 0.01 cm, the bioelectroanalytical system operates under the mixed membrane and solution transport control.

# **Acknowledgement**

This research was partially supported by Lithuanian State Science and Studies Foundation, Project No. N-08007.

- A. Svendsen, Anal. Biochem. 344, 275 (2005)
- [14] M. Puida F. Ivanauskas, I. Ignatjev, G. Valinčius, V. Razumas, Nonlinear analysis: modelling and control 12 (2), 245 (2007)
- [15] R. Verger, M.C.E. Mieras, G.H. De Haas, J. Biol. Chem. 248, 4023 (1973)
- [16] K. Kumbhakart, T. Goel, T. Mukherjee, H. Pal, J. Phys. Chem. B 108, 19246 (2004)
- [17] P. Becher, J. Phys. Chem. 66, 374 (1962)
- [18] P. Manimozhi, L. Rajendran, J. Electroanal. Chem. 647, 87 (2010)
- [19] R. Senthamarai, L. Rajendran, Electrochim. Acta. 55, 3223 (2010)
- [20] D.A. Gough, J.K Leypoldt, Anal. Chem. 51, 439 (1976)
- [21] A.A. Samarskii, The Theory of Difference Schemes (Marcel Dekker, New York – Basel, 2001)
- [22] R. Baronas, F. Ivanauskas, J. Kulys, et al., J. Math. Chem. 34, 227 (2003)
- [23] R. Baronas, J. Kulys, F. Ivanauskas, Biosens. Bioelectron. 19, 915 (2004)
- [24] R. Baronas, J. Kulys, F. Ivanauskas, J. Math. Chem. 39, 345 (2006)
- [25] R. Baronas, F. Ivanauskas, J. Kulys, Mathematical Modeling of Biosensors. An Introduction for Chemists and Mathematicians (Springer, Springer Series on Chemical Sensors and Biosensors, Dordrecht, 2010)
- [26] J.B. Raoof, R. Ojani, R. Hosseinzaden, V. Dhasemi, Anal. Sci. 19, 1251 (2003)
- [27] A.J. Bard, L.R. Faulkner, Electrochemical Methods: Fundamentals and Applications (Wiley, New York, 2001)